and

$$\ln (v_x'/v_x) = x(1 - 1/\bar{x}_n)v_2 - 2x/y - Bx \quad (31)$$

where

$$B = v_{2R}'(1 - 1/\bar{x}_{nR}') + v_{2A}'(y - 1)/\bar{x}_{nA}' \quad (32)$$

Use of eq 24 for μ_x' when $x > y$ gives

$$\ln (v_x'/v_x) = x(1 - 1/\bar{x}_n)v_2 - 2[1 + \ln (x/y)] - Bx \quad (33)$$

Substitution of eq 30 in 31 yields

$$v_x'/v_x = [(1 - v_2')/(1 - v_2)]^x = (v_1'/v_1)^x, \quad x \leq y \quad (34)$$

or

$$v_x'/v_x = \exp(-\zeta x), \quad x \leq y \quad (35)$$

where

$$\zeta \equiv -\ln [(1 - v_2')/(1 - v_2)] = B + 2/y - (1 - 1/\bar{x}_n)v_2 \quad (36)$$

Similarly, substitution of eq 30 in 33 leads to

$$v_x'/v_x = (y/ex)^2[\exp(2/y)(1 - v_2')/(1 - v_2)]^x, \quad x > y \quad (37)$$

or

$$v_x'/v_x = (y/ex)^2 \exp(\eta x), \quad x > y \quad (38)$$

where

$$\eta = 2/y - \zeta \quad (39)$$

$$\eta = (1 - 1/\bar{x}_n)v_2 - B \quad (40)$$

Defined in this manner, both ζ and η are positive. For $v_{2R}' \ll v_2$ and $(y - 1)/\bar{x}_{nA}' \ll 1$,

$$\eta \approx v_2 \quad (41)$$

and eq 38 reduces to

$$v_x'/v_x \approx (y/ex)^2 \exp(v_2 x), \quad x > y \quad (42)$$

If the anisotropic phase is taken to be ideal, as may be appropriate when $y \leq 1$ according to eq 12 or 12′, then substitution from eq 25 and 26 for the chemical potentials μ_1' and μ_x', respectively, in the equilibrium conditions expressed by eq 29 yields

$$\ln[(1 - v_2')/(1 - v_2)] = (1 - 1/\bar{x}_n)v_2 + \ln [1 - v_2'(1 - 1/\bar{x}_n')] \quad (43)$$

and

$$v_x'/v_x = x^{-2}[1 - v_2'(1 - 1/\bar{x}_n')] \exp(\eta^* x) \quad (44)$$

where

$$\eta^* = (1 - 1/\bar{x}_n)v_2 \quad (45)$$

Results of calculations of phase equilibria in polydisperse systems are presented in the three following papers.[11-13]

Acknowledgment. This work was supported by the Directorate of Chemical Sciences, Air Force Office of Scientific Research, Grant No. 77-3293.

References and Notes

(1) P. J. Flory, *Proc. R. Soc., London, Ser. A.*, **234**, 73 (1956).
(2) C. Robinson, *Trans. Faraday Soc.*, **52**, 571 (1956); C. Robinson, J. C. Ward, and R. B. Beevers, *Discuss. Faraday Soc.*, **25**, 29 (1958).
(3) J. Hermans, *J. Colloid Sci.*, **17**, 638 (1962).
(4) E. L. Wee and W. G. Miller, *J. Phys. Chem.*, **75**, 1446 (1971); W. G. Miller, J. H. Rai, and E. L. Wee, "Liquid Crystals and Ordered Fluids", Vol. 2, J. F. Johnson and R. S. Porter, Eds., Plenum Publishing Corp., New York, 1974, pp 243–255.
(5) A. Nakajima, T. Hayashi, and M. Ohmori, *Biopolymers*, **6**, 973 (1968).
(6) S. P. Papkov, *Khim. Volokna*, **15**, 3 (1973); S. P. Papkov, V. G. Kalichikhin and V. D. Kalmykova, *J. Polym. Sci., Polym. Phys. Ed.*, **12**, 1753 (1974).
(7) P. W. Morgan, *Polym. Prepr., Am. Chem. Soc., Div. Polym. Chem.*, **17**, 47 (1976).
(8) S. L. Kwolek, P. W. Morgan, J. R. Schaefgen, and L. W. Gulrich, *Polym. Prepr., Am. Chem. Soc., Div. Polym. Chem.*, **17**, 53 (1976).
(9) P. J. Flory, *J. Am. Chem. Soc.*, **87**, 1833 (1965); A. Abe and P. J. Flory, *ibid.*, **87**, 1838 (1965).
(10) P. J. Flory, *Discuss. Faraday Soc.*, **49**, 7 (1970).
(11) A. Abe and P. J. Flory, *Macromolecules*, companion paper in this issue, part 2.
(12) P. J. Flory and R. S. Frost, *Macromolecules*, companion paper in this issue, part 3.
(13) R. S. Frost and P. J. Flory, *Macromolecules*, companion paper in this issue, part 4.

Statistical Thermodynamics of Mixtures of Rodlike Particles. 2. Ternary Systems

Akihiro Abe and Paul J. Flory*

Department of Chemistry, Stanford University, Stanford, California 94305.
Received June 8, 1978

ABSTRACT: Phase equilibria have been calculated for athermal, three-component systems comprising a solvent with axis ratio $x_1 = 1$ and two solutes consisting of rodlike particles with axis ratios x_a and x_b, respectively, equal to (40,20), (100,20), and (100,10). The small immiscibility gaps separating the isotropic (dilute) from the anisotropic (more concentrated) phase in the respective two-component systems (1,a) and (1,b) are enlarged by addition of the second solute component. The species a and b, with $x_a > x_b$, occur preferentially in the anisotropic and isotropic phases, respectively. The component with axis ratio $x_a = 100$ is virtually excluded from the isotropic phase when the amount of the smaller component ($x_b = 10$ or 20) in the system is more than a few percent of a. Triphasic equilibria are predicted for the systems $x_a,x_b = 100,20$ and 100,10.

In this paper we apply the relationships derived in the one preceding[1] (referred to as 1) to systems consisting of two rigid, rodlike solutes having unequal axis ratios, x_a and x_b, and a solvent. As in 1, the breadths of the solute molecules are taken to be the same and equal to the diameter of the isodiametric solvent. The systems are considered to be athermal. The straightforward extensions of the theory that would be required to take account of exchange interactions upon mixing are deliberately disregarded.

0024-9297/78/2211-1122$01.00/0

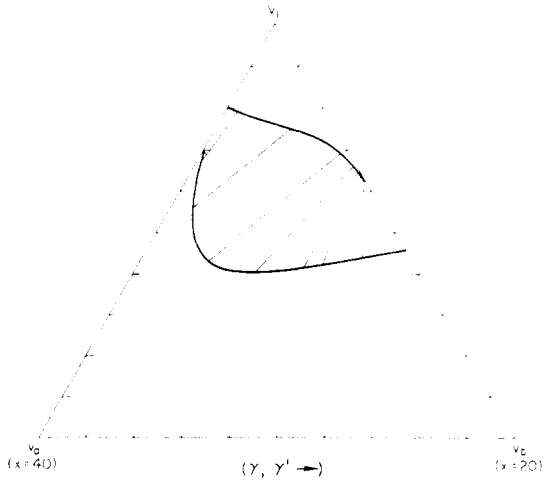

Figure 1. Ternary phase diagram calculated for solvent and two rodlike solutes with axis ratios $x_1 = 1$, $x_a = 40$, and $x_b = 20$, respectively. Coordinates are volume fractions.

Concentrations in the two phases at equilibrium were calculated for selected values of x_a and x_b, with $x_a > x_b$, and of the fraction γ' of the solute in the anisotropic phase that consists of component b, i.e.,

$$\gamma' = v_b'/v_2' \tag{1}$$

The number average $\bar{x}_n'$ in the anisotropic phase is determined by these three quantities through the relation

$$1/\bar{x}_n' = (1 - \gamma')/x_a + \gamma'/x_b \tag{2}$$

The required numerical solutions were obtained according to the following procedure: (i) A trial value of v_2' was chosen, and v_b', $v_a' = v_2' - v_b'$, and $\bar{x}_n'$ were evaluated from γ' and v_2' by use of eq 1 and 2. (ii) The disorder parameter y was evaluated using either eq 1-12 or 1-12′. Use of the latter equation requires the substitutions $v_{2A}' = v_2'$ and $\bar{x}_{nA}' = \bar{x}_n'$ if $y < x_b$; if $y \geq x_b$, then $v_{2A}' = v_a'$ and $\bar{x}_{nA}' = x_a$. (iii) According to eq 1-37,

$$v_a = v_a'(y/ex_a)^{-2}[\exp(-2/y)(1 - v_2)/(1 - v_2')]^{x_a} \tag{3}$$

and, for $y < x_b$,

$$v_b = v_b'(y/ex_b)^{-2}[\exp(-2/y)(1 - v_2)/(1 - v_2')]^{x_b} \tag{4}$$

For $y \geq x_b$, eq 1-34 gives

$$v_b = v_b'[(1 - v_2)/(1 - v_2')]^{x_b} \tag{5}$$

The sum of eq 3 and 4, or of eq 3 and 5 if $y \geq x_b$, gives an equation that was solved by trial for $v_2 = v_a + v_b$. Then v_a, v_b, and $\bar{x}_n$ were calculated for the isotropic phase. (iv) The chemical potential $(\mu_1 - \mu_1^0)'/RT$ of the solvent in the anisotropic phase was calculated according to eq 1-22 from $v_{2A}' = v_2'$, $v_{2R}' = 0$, $\bar{x}_{nA}' = \bar{x}_n'$, and y if $y < x_b$, or from $v_{2A}' = v_a'$, $v_{2R}' = v_b'$, $\bar{x}_{nA}' = x_a$, $\bar{x}_{nR}' = x_b$, and y if $y \geq x_b$. The result was compared with $(\mu_1 - \mu_1^0)/RT$ for the isotropic phase calculated from v_2 and $\bar{x}_n$ according to eq 1-27. (v) Another trial v_2' was chosen and the steps (i)–(iv) were repeated, and so on until the condition $\mu_1 = \mu_1'$ was satisfied.

Phase Equilibria in Ternary Systems

Calculations have been performed for the athermal systems comprising a solvent and two rodlike solute components with axis ratios $(x_a,x_b) = (40,20)$, (100,20), and (100,10). Results for these systems are presented in the stated order.

The System: $x_a = 40$, $x_b = 20$. The calculated ternary phase diagram is shown in Figure 1. Binodials delineating the boundaries of the biphasic region are heavy lined. The upper curve represents the isotropic phase, the lower the anisotropic phase. The immiscibility gaps for the parent binary systems consisting of one or other of the solutes and the solvent occur on the respective lateral axes that meet at the apex for solvent (component 1). Representative tie lines for conjugate phases in the ternary system are shown by light lines.

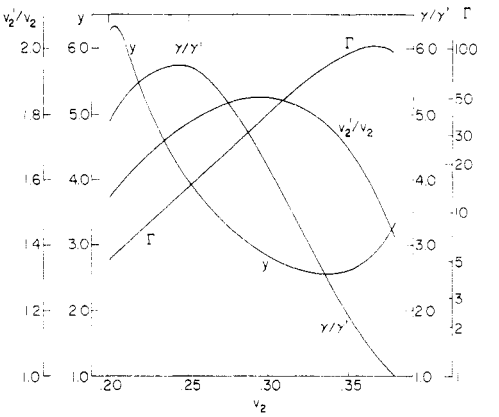

Figure 2. Plots of v_2'/v_2, y, γ/γ', and Γ (see eq 6) against the combined volume fraction v_2 of solutes in the isotropic phase for the system (40,20).

Several significant features command attention. First, the biphasic region, i.e., the miscibility gap, is widened by mixing either solute component with the other. Second, the diagram is highly unsymmetric with respect to the two solute components. This is shown most strikingly by the large inclinations of the tie lines to the straight lines that may be drawn from the vertex v_1 to the conjugate phase points. Extension of these lines would subdivide the base line $v_a \cdots v_b$ into segments with lengths in the ratios $(1 - \gamma)/\gamma = v_a/v_b$ and $(1 - \gamma')/\gamma' = v_a'/v_b'$, respectively. Thus, the ratios of the two solutes in the coexisting phases differ markedly; the larger component, a, occurs preferentially in the anisotropic phase, and the smaller one, b, in the isotropic phase.

These features are shown more fully in Figure 2. Here we choose v_2 as independent variable, principally because it alone of the various quantities associated with the equilibria varies monotonically with over-all composition. The ratio v_2'/v_2 of the combined solute concentrations in the two phases quantitates the broadening of the immiscibility gap with mixing of the two solutes. It reaches a maximum of 1.85 compared to 1.52 and 1.43 for the respective binary systems,[2] (1,a) and (1,b).

The quantity $\gamma/\gamma' = (v_b/v_2)/(v_b'/v_2')$, being the ratio of the intercepts of the two straight lines drawn from the vertex v_1 through the termini of the tie line and extended to the base line $v_a \cdots v_b$, affords an index of the partitioning of the solute components between the two phases. This ratio, as shown in Figure 2, rises to values in excess of five at intermediate compositions. It fails as a satisfactory measure of partitioning of the components at higher solute concentrations where maintenance of phase equilibrium requires a high proportion of the species b of lower axis ratio. In this limit both γ and γ', and hence their ratio as well, approach unity.

The quantity

$$\Gamma = \gamma(1 - \gamma')/\gamma'(1 - \gamma) = (v_b/v_a)/(v_b'/v_a') \tag{6}$$

is a more satisfactory measure of the preferential apportionment of the two species between the two phases. In order to accommodate the large changes in this quantity with v_2, Γ is plotted on a logarithmic scale in this figure and in others to follow. It rises to high values in Figure

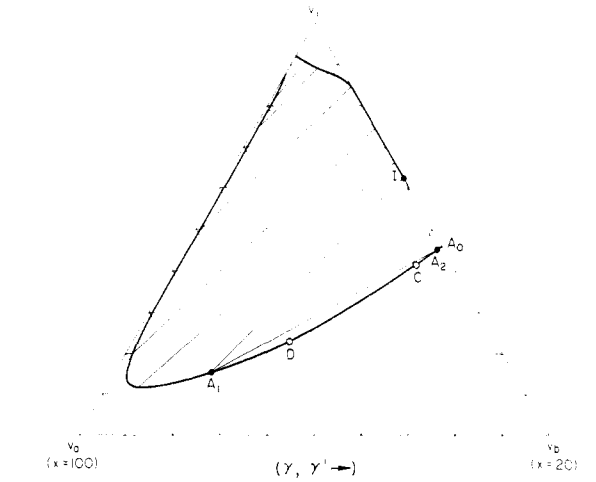

Figure 3. Ternary phase diagram calculated for the system (100,20); see legend to Figure 1. Coexisting phases at triphasic equilibrium are shown by filled circles at I (isotropic), A_1 (anisotropic), and A_2 (anisotropic). Points C and D are termini of tie lines joining extrema I_C and I_D of the metastable binodials shown in Figure 4; see text.

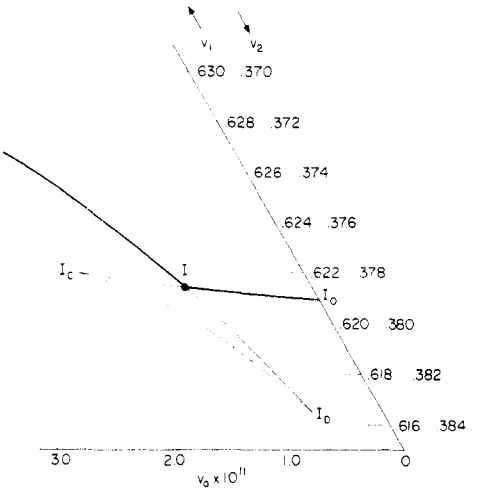

Figure 4. Enlarged plot of the binodials in the vicinity of the isotropic phase (I) in equilibrium with two anisotropic phases (A_1 and A_2) in the system (100,20); see Figure 3. Binodials for isotropic phases in metastable equilibrium with an anisotropic phase are dashed.

2 when the solute consists of a preponderance of component b. The concentration of the larger component a in the isotropic phase is then very low. Over most of the range, log Γ is approximately linear with v_2. This observation may be shown[3] to follow from the equations expressing the volume fraction ratios v_x'/v_x and given in 1.

We also show y plotted against v_2 in Figure 2. Its dependence on composition as represented by v_2 is somewhat complex. As expected, however, it tends to decrease as the proportion of b increases. For all compositions of this two-phase system $1 < y < x_b$.

The System: $x_a = 100$, $x_b = 20$. The phase diagram for this system is shown in Figure 3. The features revealed in Figure 1 for the system (40,20) are accentuated here. For γ' in the approximate range $0.0133 < \gamma' < 0.0252$ the equations yield three solutions, as is apparent from the binodial for the anisotropic phase. The binodial for the isotropic phase merges into the $v_1 \cdots v_b$ axis. At volume fractions $v_2 = 1 - v_1$ exceeding 0.30, the volume fraction v_a in that phase is $<10^{-7}$ and it falls to $\sim 10^{-10}$ at $v_2 \approx v_b = 0.35$.

Most remarkable is the presence of a region of composition for the system as a whole which yields three coexisting phases. These phases are indicated by filled circles labeled I (isotropic), A_1 (anisotropic), and A_2 (anisotropic). The triangle defined by these points is the triphasic region.

The portion of the diagram in the neighborhood of point I in Figure 3 is shown on a greatly enlarged scale in Figure 4. The line I_0I joining the composition I_0 for the isotropic phase in the binary system (1,b) with the isotropic phase point I for the three-phase, three-component system is the locus of the upper termini of tie lines that extend downwards to the conjugate anisotropic phases along the line segment A_2A_0 in Figure 3. The heavy line extending above point I in Figure 4 shows a small portion of the binodial for the isotropic phase shown in full in Figure 3. It is the locus of termini of tie lines that meet the binodial for the anisotropic phase in Figure 3 to the left of point A_1, as shown in that figure.

The succession of tie lines commencing on line segment I_0I continues beyond those that originate within this interval. The locus of the upper termini of this family of tie lines extends to I_C in Figure 4. The tie line from I_C joins point C in Figure 3. Similarly, the family of tie lines originating at points on the upper heavy line includes also the subset of tie lines commencing in the interval I to I_D. The tie line from I_D meets the binodial for the anisotropic phase at point D in Figure 3. Tie lines terminating on line segment CD in Figure 3 originate on line segment I_CI_D in Figure 4. The lines II_C, II_D, and I_CI_D are dashed in Figure 4 inasmuch as they represent metastable states. This follows from the fact that the tie lines extending therefrom intersect the tie lines from the heavy solid lines in Figure 4. The point I was located as the intersection of loci I_0I_C with the upper curve. The points A_1 and A_2 (Figure 3) were then established as the termini of the two tie lines originating at I.

Table I
Compositions and Molecular Parameters for the Three Coexisting Phases in the System: $x_a = 100$, $x_b = 20$

	isotropic phase I	anisotropic phase A_1	anisotropic phase A_2
v_2	0.3786	0.8488	0.5517
v_a	0.1109×10^{-10}	0.6407	0.0177
v_b	0.3786	0.2081	0.5340
$\bar{x}_n$	20.00	50.49	20.53
y		1.130	3.187

Compositions for the three coexisting phases and the disorder parameters y for the two anisotropic phases are recorded in Table I.

An additional set of tie lines, not shown in Figure 3, occupies the region bounded by curve A_1DCA_2 and tie line A_1A_2. They represent stable biphasic equilibria between two anisotropic phases.

The quantities v_2'/v_2, γ/γ', Γ, and y for this system are shown as functions of v_2 in Figure 5. The dependences of these quantities on v_2 resemble those shown in Figure 2 for the system $x_a = 40$, $x_b = 20$, but their changes with composition are more pronounced. The partitioning ratio Γ is plotted on a compressed logarithmic scale. Again log Γ is approximately linear with v_2.[3] The continuation of the curve for v_2'/v_2 into the metastable region is shown as a dashed line. For all compositions, $y < x_b$. At $v_2 = 0.35$, the disorder parameter y exhibits a minimum value of 0.975. The transgression of the physical limit $y = 1$, being very small, has been disregarded; see below.

The System: $x_a = 100$, $x_b = 10$. The phase diagram for this system is shown in Figure 6. The solid lines

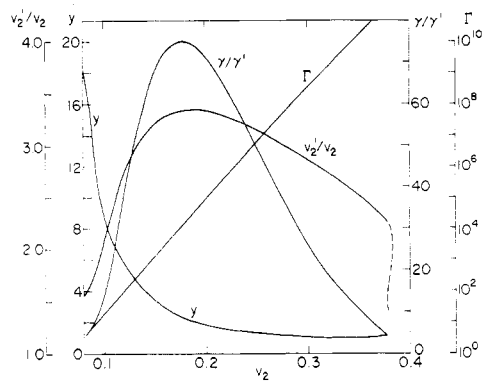

Figure 5. Characteristics of biphasic equilibria in the system (100,20) plotted against v_2 for phases joined by tie lines above IA_1 in Figure 3. The extension of the curve for v_2'/v_2 into the metastable range is dashed.

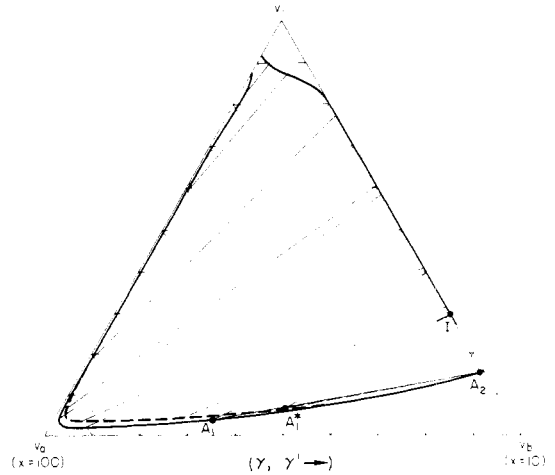

Figure 6. Ternary phase diagram calculated for the system (100,10); see legend to Figure 1. Binodials and tie lines calculated without restriction on y are shown by solid lines; coexisting phases thus calculated at triphasic equilibrium are I, A_1, and A_2. The binodial for the anisotropic phase calculated with $y = 1$ and associated tie lines are dashed; coexisting phases at triphasic equilibrium are I, A_1*, and A_2 (approximately; see Table II).

represent results of calculations carried out as described above, values of y less than unity being employed where eq 1-12 (or 1-12′) so indicates, cf. seq. The points thus calculated for triphasic equilibrium are those labeled, I, A_1, and A_2, as in Figure 3. They were determined as described above for the system (100,20). Coordinates of these points calculated in the manner stated are given in the upper portion of Table II, values of $\bar{x}_n$ and y being included. As for the preceding system, the equations yield three solutions within a small range of γ' which in this case is approximately $0.0042 < \gamma' < 0.0610$.

The quantities v_2'/v_2, γ/γ', Γ, and y are plotted against v_2 in Figure 7. The principal features observed for the system (100,20) are reiterated here, some of them being more marked than for that system. The ratio v_2'/v_2 that is indicative of the breadth of the phase gap rises to a maximum comparable in magnitude to that in Figure 5, but the curve is more sharply peaked. The ratio γ/γ' also rises more sharply and it exhibits a higher maximum. Most striking is the steep increase of Γ with v_2. This is a reflection of the falling concentration v_a of the larger species in the isotropic phase. At $v_2 = 0.40$, $v_a \approx 10^{-10}$; at $v_2 = 0.71$, v_a falls to $\approx 10^{-23}$. Thus, exclusion of component a from this phase becomes virtually complete; see also Table II.

The value of y (see Figure 7) exceeds $x_b = 10$ for $v_2 < 0.107$. In this range, therefore, $v_{2R}' > 0$ and use of eq 5

Table II
Compositions and Molecular Parameters for the Three Coexisting Phases in the System: $x_a = 100$, $x_b = 10$

	isotropic phase I or I*	anisotropic phase A_1 or A_1*	anisotropic phase A_2 or A_2*
Calculated without Restrictions on y (See Text)			
v_2	0.7058	0.9638	0.8499
v_a	0.80×10^{-23}	0.6393	0.0074
v_b	0.7058	0.3245	0.8425
$\bar{x}_n$	10.00	24.81	10.08
y		0.730	1.590
Calculated with $y = 1$ as Lower Limit (See Text)			
v_2	0.7058	0.9353	0.8505
v_a	1.03×10^{-23}	0.4639	0.0100
v_b	0.7058	0.4714	0.8405
$\bar{x}_n$	10.00	18.06	10.11
y		1.000	1.583

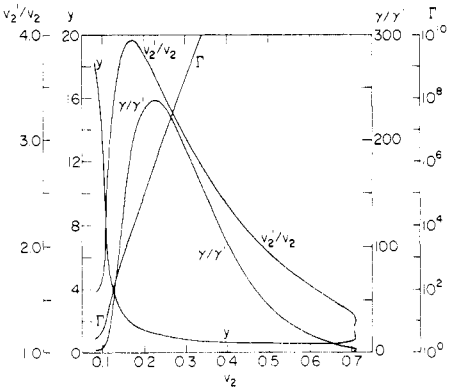

Figure 7. Characteristics of biphasic equilibria in the system (100,10) plotted against v_2 for phases joined by tie lines above tie line IA_1 in Figure 6.

rather than eq 4 was obligatory. Over the range $v_2 = 0.27$ ($v_2' = 0.88$) to $v_2 = 0.710$ ($v_2' = 0.925$) the value of y falls below unity; see Figure 7. It reaches a minimum of 0.55 at $v_2 \approx 0.60$.

In consideration of the physical unacceptability of $y < 1$ according to strict interpretation of the model,[1,2] we repeated the calculations with y set equal to unity whenever eq 1-12, or 1-12′, yielded $y < 1$. In place of the equations used above, the partitioning of the solute components was calculated according to eq 1-44 derived assuming ideal mixing in the anisotropic phase, in keeping with the reduction of the mixing partition function to the ideal mixing law when $y = 1$.[1,2] Results of these calculations are shown by the dashed lines in Figure 6. The binodial for the isotropic phase is not affected perceptibly by this revision. The binodial for the anisotropic phase is raised slightly over the range in which $y < 1$ according to eq 1-12. Directions of tie lines are not altered significantly. However, the location of phase A_1 is shifted to A_1* as a consequence of the small displacement of the binodial for the anisotropic phase. The point A_2 is shifted slightly to the left, but the change is too small to be discernible in Figure 6. The coordinates of these points are given in the lower portion of Table II.

Thus, the only significant effect of restricting y to the range $y \geq 1$ in the foregoing manner is the displacement of the phase point A_1 for triphasic equilibrium to A_1*. This alteration is appreciable owing to the extreme sensitivity of the tie line intersections to the location of the binodial for the anisotropic phase, the directions of the tie lines being little affected as noted above.

Acknowledgment. This work was supported by the Directorate of Chemical Sciences, Air Force Office of

Scientific Research, Grant No. 77-3293.

References and Notes

(1) P. J. Flory and A. Abe, *Macromolecules*, companion paper in this issue, part 1.
(2) P. J. Flory, *Proc. R. Soc. London, Ser. A.*, **234**, 73 (1956).
(3) It follows from eq 1-35, -38-40, and -32 that $\ln \Gamma \approx \eta (x_a - x_b)$ for $(x_a - x_b) \gg 1$. Moreover, as eq 1-41 indicates, $\eta \approx v_2$. Numerical calculations confirm this approximation, except at volume fractions v_2 approaching the upper limit for $\gamma = 1$, where the approximation fails altogether. Hence log Γ should be very nearly linear in v_2 over most of the range, as the computations shown in Figures 2, 5, and 7 confirm for the systems investigated.

Statistical Thermodynamics of Mixtures of Rodlike Particles. 3. The Most Probable Distribution

Paul J. Flory* and Randall S. Frost

Department of Chemistry, Stanford University, Stanford, California 94305.
Received June 8, 1978

ABSTRACT: Biphasic equilibria are investigated for athermal mixtures in which the solute comprises rodlike particles having the familiar distribution $v_x^0 = v_2^0(1-p)^2xp^{x-1}$, x being both the number of units and the axis ratio. Under conditions such that the volumes of the coexisting phases are comparable, the polydispersity in each phase is considerably lower than for the parent ("most probable") distribution. Fractionation between the phases is remarkably efficient. A concomitant of the preferential partitioning of lower and higher species between the respective phases is the broad range of overall concentration within which the system is biphasic. The undiluted polydisperse solute is predicted to be biphasic for $(1-p)^{-1}$ in the range ~2.3–17.5. It is isotropic below this range and wholly anisotropic for greater average chain lengths $\bar{x}_n^0$. According to theory, an isotropic phase in which the solute retains the foregoing distribution can coexist in equilibrium with an anisotropic (nematic) phase only if this phase comprises species of very large x at high concentration in ordered array. This deduction follows regardless of the average $\bar{x}_n^0 = (1-p)^{-1}$ in the isotropic phase provided only that $\bar{x}_n^0 > 2.3$. If interchange processes $M_{x_1} + M_{x_2} \rightleftarrows M_{x_1+x_2}$ occur freely at random, continuous transformation to a highly ordered anisotropic phase is predicted. Thus, formation of rodlike particles through random, linear aggregation of subunits offers an exceptionally simple scheme for self-ordering.

In this paper we treat the partitioning of a so-called "most probable" distribution of rodlike particles between isotropic and anisotropic phases. As in the preceding papers, 1[1] and 2,[2] exchange interactions between solute particles are assumed to be null. Hence, only the spaciogeometric requirements of the solute particles are considered.

The most probable distribution for particles consisting of x units is specified by

$$v_x^0/v_2^0 = (1-p)^2xp^{x-1} \tag{1}$$

where p may be considered to be the expectation of perpetuation of a sequence of units to include at least one more unit, $1-p$ being the expectation of termination of the sequence. The zero superscripts signify the unpartitioned distribution; v_2^0 denotes the mean volume fraction of solute in both phases combined, and v_x^0 the corresponding volume fraction of species x in the system as a whole. The number average size, or axis ratio, is

$$\bar{x}_n^0 \equiv \sum v_x^0/\sum x^{-1}v_x^0 = (1-p)^{-1} \tag{2}$$

Theoretical Relationship for Phase Equilibria

1. Equations of Conservation. Let V and V' denote the volumes of the isotropic and anisotropic phases, respectively; v_2 and v_2' will denote the respective volume fractions of solute in these phases. Then

$$\Phi v_2 + (1-\Phi)v_2' = v_2^0 \tag{3}$$

where Φ is the ratio of the volume of the isotropic phase to the total volume, i.e.,

$$\Phi = V/(V+V') = V/V^0 \tag{4}$$

Similarly,

$$\Phi v_x + (1-\Phi)v_x' = v_x^0 \tag{5}$$

Hence, for the distribution considered (see eq 1)

$$\Phi v_x + (1-\Phi)v_x' = v_2^0(1-p)^2xp^{x-1} \tag{5'}$$

Also

$$\Phi v_2/\bar{x}_n + (1-\Phi)v_2'/\bar{x}_n' = v_2^0/\bar{x}_n^0 = v_2^0(1-p) \tag{6}$$

2. Systems at Equilibrium Disorder ($y = y_{eq}$). In this most general case we take $y = y_{eq}$, disregarding the possibility that y_{eq} may be less than unity.[1,2]

Consider first the solute species with $x \leq y$, where $y = y_{eq} > 1$. Substitution from eq 1-35 for v_x in eq 5′ gives

$$v_x'/v_2^0 = \Phi^{-1}(1-p)^2xp^{x-1}/[e^{\zeta x} + (1-\Phi)\Phi^{-1}], \quad x \leq y \tag{7}$$

ζ being defined by eq 1-36. Hence,

$$v_{2R}'/v_2^0 = \Phi^{-1}(1-p)^2I_{1R} \tag{8}$$

where

$$I_{1R} = \sum_1^{x\leq y} xp^{(x-1)}/[e^{\zeta x} + (1-\Phi)\Phi^{-1}] \tag{9}$$

The number average of x for species in this category is

$$\bar{x}_{nR}' = I_{1R}/I_{0R} \tag{10}$$

where

$$I_{0R} = \sum_1^{x\leq y} p^{x-1}/[e^{\zeta x} + (1-\Phi)\Phi^{-1}] \tag{11}$$

Similarly for species with x exceeding y we have from eq 5′ and 1-38

$$v_x'/v_2^0 = \Phi^{-1}(y/e)^2(1-p)^2xp^{x-1}/[x^2e^{-\eta x} + (y/e)^2(1-\Phi)\Phi^{-1}], \quad x > y \tag{12}$$

η being defined by eq 1-39 or 1-40. Then

0024-9297/78/2211-1126$01.00/0